Pflugers Arch - Eur J Physiol (2011) 461:123–139
DOI 10.1007/s00424-010-0884-3

NEUROSCIENCE

Effect of a temperature increase in the non-noxious range on proton-evoked ASIC and TRPV1 activity

Maxime G. Blanchard · Stephan Kellenberger

Received: 23 June 2010 / Revised: 15 September 2010 / Accepted: 15 September 2010 / Published online: 6 October 2010

Abstract Acid-sensing ion channels (ASICs) are neuronal H^+-gated cation channels, and the transient receptor potential vanilloid 1 channel (TRPV1) is a multimodal cation channel activated by low pH, noxious heat, capsaicin, and voltage. ASICs and TRPV1 are present in sensory neurons. It has been shown that raising the temperature increases TRPV1 and decreases ASIC H^+-gated current amplitudes. To understand the underlying mechanisms, we have analyzed ASIC and TRPV1 function in a recombinant expression system and in dorsal root ganglion (DRG) neurons at room and physiological temperature. We show that temperature in the range studied does not affect the pH dependence of ASIC and TRPV1 activation. A temperature increase induces, however, a small alkaline shift of the pH dependence of steady-state inactivation of ASIC1a, ASIC1b, and ASIC2a. The decrease in ASIC peak current amplitudes at higher temperatures is likely in part due to the observed accelerated open channel inactivation kinetics and for some ASIC types to the changed pH dependence of steady-state inactivation. The increase in H^+-activated TRPV1 current at the higher temperature is at least in part due to a hyperpolarizing shift in its voltage dependence. The contribution of TRPV1 relative to ASICs to H^+-gated currents in DRG neurons increases with higher temperature and acidity. Still, ASICs remain the principal pH sensors of DRG neurons at 35°C in the pH range ≥6.

Keywords Ligand-gated · Ion channel · DRG neurons · Acidification · ASIC · TRPV1 · pH dependence · Temperature · Dorsal root ganglion · Acidosis · TRP channels

Abbreviations

AP	Action potential
ASIC	Acid-sensing ion channel
BCTC	4-(3-Chloro-2-pyridinyl)-*N*-[4-(1,1-dimethylethyl)phenyl]-1-piperazinecarboxamide
CHO	Chinese hamster ovary
DRG	Dorsal root ganglia
ENaC	Epithelial sodium channel
HEK	Human embryonic kidney
nH	Hill number
$pH_{0.5}$	pH of half-maximal activation
$pHIn_{0.5}$	pH of half-maximal inactivation
SSIN	Steady-state inactivation
τ_I	Time constant of open channel inactivation
τ_R	Time constant of recovery from inactivation
TRPV1	Transient receptor potential vanilloid 1
$V_{0.5}$	Voltage of half-maximal conductance
V_m	Membrane potential

Introduction

Acid-sensing ion channels (ASICs) are neuronal H^+-gated Na^+ channels that are members of the epithelial Na^+ channel (ENaC)/degenerin family of ion channels [24, 54]. Functional ASICs are homo- or heterotrimers of ASIC1a, ASIC1b, ASIC2a, ASIC2b, and/or ASIC3 subunits [14, 20, 54]. ASIC2b is not functional as homomultimer but can form functional heteromeric channels with other subunits [27]. ASIC4 channel activity has not been

Electronic supplementary material The online version of this article (doi:10.1007/s00424-010-0884-3) contains supplementary material, which is available to authorized users.

M. G. Blanchard · S. Kellenberger (✉)
Département de Pharmacologie et de Toxicologie,
Université de Lausanne,
Rue du Bugnon 27,
1005 Lausanne, Switzerland
e-mail: Stephan.Kellenberger@unil.ch

detected so far. It may participate in regulating the membrane availability of other ASIC subunits [11]. Transient receptor potential vanilloid 1 (TRPV1) is a Ca^{2+}-permeable multimodal ion channel activated by low pH (≤6.0), noxious heat (>43°C), capsaicin, and voltage and is a member of the subfamily of temperature-dependent transient receptor potential channels [6, 25, 39].

Both ASICs and TRPV1 are expressed in small diameter dorsal root ganglion (DRG) neurons giving rise to slowly conducting Aδ and C fibers which are believed to be nociceptors [26]. A previous study from our laboratory found co-expression of ASICs with nociceptor markers in this subpopulation of DRG neurons [35]. Since ASICs and TRPV1 are both H^+-activated channels, they are good candidates to serve as H^+ sensors in nociceptors. Studies with ASIC knockout mice indicated that ASIC3 is the main ASIC subunit of the peripheral nervous system involved in inflammatory and acid-induced pain sensation [7, 37, 38]. The exact role of ASICs—i.e., pronociceptive or modulatory—is, however, not clear and likely depends on factors that are currently not understood. In human skin, ASICs mediate the pain that is felt when acidic solutions are injected or applied by iontophoresis [21, 44]. Robust hypersensitivity to heat can develop with inflammation or after injection of specific inflammation mediators, and this sensitization is abolished in TRPV1-deficient mice [5, 9]. This supports an important role of TRPV1 in thermal hyperalgesia.

Numerous studies have described H^+-induced currents mediated by ASICs and TRPV1 in sensory neurons [5, 32, 34, 35]. However, most of these studies were carried out at room temperature. TRPV1 is activated by both noxious temperature and acidic pH, and it had previously been shown that acidification shifts the TRPV1 temperature dependence to lower values [22, 42]. As expected, the amplitude of the H^+-induced TRPV1-like current in DRG neurons increased with temperature [32]. For ASICs, in contrast, it had been shown that peak current amplitudes are decreased or unchanged and that the open channel inactivation time course is accelerated with increasing temperature [1, 32]. The mechanisms underlying this different regulation of ASICs and TRPV1 by temperature are not known. We reasoned that temperature might influence the pH dependence and other functional parameters of these channels and thereby change ASIC and TRPV1 current amplitudes. To our knowledge, the temperature dependence of H^+-gated ASIC and TRPV1 currents in DRG neurons has so far been shown at one single pH [1, 32]. Variation of the temperature may affect the contribution of ASICs and TRPV1 to the acid-induced current in sensory neurons in a way that depends on the pH. To answer these open questions, we have characterized H^+-gated ASIC and TRPV1 currents at 25°C and 35°C in transfected cells and in DRG neurons. We chose 35°C since this is close to the temperature at the body surface, where many peripheral sensors are located. We show that the increase in temperature leads to an acceleration of open channel inactivation of all ASICs, reduces the current amplitude of ASIC1a and ASIC1b, and increases the TRPV1 current amplitude, but has only minor effects on ASIC and TRPV1 pH dependence. In small diameter DRG neurons, the ratio of current amplitude and charge transfer between TRPV1 and ASICs increased with acidic pH and temperature. The acid-induced depolarization at pH ≥6 under current clamp was decreased with increasing temperature in a subpopulation of neurons.

Materials and methods

DRG neuron isolation and culture

Adult male Wistar rats (Janvier, Le Genest Saint Isle, France) were killed using CO_2 for experiments involving DRG neurons. All experimental procedures were carried out according to the Swiss Federal Law on Animal Welfare and approved by the Committee on Animal Experimentation of the Canton de Vaud [55]. DRG neuron isolation and culture were performed as previously described [35]. Briefly, rats were killed using CO_2 and lumbar DRGs were removed bilaterally. The isolated DRG were incubated at 37°C for 2 h in Neurobasal A medium (Invitrogen, Basel, Switzerland) containing type P collagenase (0.125%, Roche, Basel, Switzerland) and trypsinized (0.25%, Invitrogen) 30 min at 37°C in divalent-free PBS solution. Following enzymatic digestion, ganglia were triturated with a fire-polished Pasteur pipette and the dissociated neurons were plated on high molecular weight poly-lysine (0.1 mg/ml, mol wt >300,000, Sigma, Buchs, Switzerland)-coated coverslips. Neurons were held at 37°C overnight, and medium was replaced the following morning with L15 Leibovitz medium (Invitrogen) supplemented with 10% fetal calf serum (FCS, GIBCO), 5 mM HEPES, pH adjusted to 7.4 with NaOH and osmolarity adjusted to 320 using sucrose. Neurons were kept at 4°C and used within 48 h of plating [4].

Recombinant expression of ASICs and TRPV1

Previously described cell lines stably expressing mouse ASIC1a (the mouse ASIC1a protein sequence is 99.8% identical to rat ASIC1a), rat ASIC1b, human ASIC2a (99% identical to rat ASIC2a), and rat ASIC3 were used in the present experiments [35]. cDNA encoding rat TRPV1 was subcloned into the pEAK8 expression vector (EdgeBio, Gaithersburg, USA) which contains a gene for puromycine

resistance. Chinese hamster ovary cells (CHO) were cotransfected with the TRPV1-peak8 construct and the green fluorescent protein using Lipofectamine 2000 (Invitrogen). At day 4 post transfection, 10 μg/ml puromycine (PAA, Pasching, Austria) was added to the medium. Selection occurred during 2 weeks before cells were used in electrophysiological experiments. Cells were grown in DMEM/F12 medium (GIBCO) supplemented with 5% FCS and 1% penicillin/streptomycin. Human embryonic kidney cells (HEK) were transfected with the TRPV1-peak8 construct and grown in DMEM (GIBCO) supplemented with 10% FCS and 1% penicillin/streptomycin. Transfected cells were passaged 24–48 h prior to the experiments onto poly-lysine-coated coverslips.

Electrophysiological measurements

Electrophysiological measurements were carried out with an EPC 10 patch clamp amplifier (HEKA Electronics, Lambrecht, Germany). Data acquisition and analysis were performed using HEKA's Patchmaster and Fitmaster software. The sampling interval was set to 0.5–1 ms for voltage clamp experiments of ASIC and TRPV1 currents and filtering was set to 3 kHz in all experiments. Experiments were carried out with the whole-cell patch clamp technique. Fast solution exchange (~100 ms) was achieved using the cF-8VS computer-controlled electro valve assembly and the MPRE8 perfusion system (Cell MicroControls, Norfolk, VA, USA). Pipettes were pulled from borosilicate glass (World Precision Instruments, Stevenage, UK) and had resistance between 2 and 6 MΩ, when filled with the pipette solution. Series resistance compensation was set to 50–95% in all voltage clamp experiments. Voltage clamp experiments were performed at a holding potential of −60 mV. In current clamp experiments, current was injected to obtain a membrane potential of −60 mV at the beginning of the experiment. The neuron diameter was estimated from the average of the longest and shortest axes as measured through an eyepiece micrometer scale. Only small diameter DRG neurons (<30 μm) were included in the study.

Solutions

Pipette solutions were adapted to the different types of measurements and contained for measurement of recombinant ASICs (in mM) 90 CsOH, 90 gluconic acid, 10 NaCl, 10 KCl, 1 $MgCl_2$, 60 *N*-2-hydroxyethylpiperazine-*N*-2-ethanesulfonic acid (HEPES), and 10 ethyleneglycoltetraacetic acid (EGTA), pH adjusted to 7.3 with CsOH. Pipette solution for measurement of recombinant TRPV1 contained (in mM) 140 CsCl, 5 EGTA, and 10 3-(*N*-morpholino)propanesulfonic acid (MOPS), pH adjusted to 7.4 with CsOH [42]. Pipette solution for voltage clamp experiments in DRG neurons contained (in mM) 100 CsOH, 100 gluconic acid, 10 NaCl, 1 $MgCl_2$, 60 HEPES, 10 EGTA, 2 adenosine triphosphate (ATP), and 0.3 guanosine triphosphate (GTP), pH adjusted to 7.3 with CsOH. Pipette solution for voltage clamp experiments of TRPV1 characterization in DRG neurons contained (in mM) 100 CsOH, 100 gluconic acid, 5 $MgCl_2$, 40 HEPES, 10 BAPTA, 2 ATP, and 0.3 GTP, pH adjusted to 7.3 with CsOH. Current clamp experiments in DRG neurons were performed with pipette solution containing (in mM) 90 K-gluconate, 10 KCl, 10 NaCl, 1 $MgCl_2$, 60 HEPES, 2 ATP, and 0.3 GTP, pH adjusted to 7.3 using NaOH. Extracellular solutions contained (in mM) 140 NaCl, 4 KCl, 2 $CaCl_2$, 1 $MgCl_2$, 20 MOPS, and 10 glucose, pH adjusted to the desired value using NaOH/HCl. Extracellular solutions for the characterization of TRPV1 contained (in mM) 140 NaCl, 4 KCl, 2 $MgCl_2$, 20 MOPS, and 10 glucose, pH adjusted with NaOH/HCl; and either 1.1 $CaCl_2$, 10 EGTA (DRG neurons), or 1 EGTA (cloned TRPV1). The MOPS buffer was used throughout the experiments for extracellular solutions because of its low pH buffering temperature dependence. Depending on the literature source, the ΔpK/10°C of MOPS is between −0.013 and −0.06 [15, 30]. Despite good temperature buffering capability, the pH of all our solutions was measured at different temperatures on a bench top temperature-corrected pH meter (Seven Easy, Mettler Toledo, Greifensee, Switzerland), and the experimental pH values were corrected for the observed shift. In all cases, solutions were slightly more acidic at higher temperature. This difference was less than 0.1 pH units in the pH range 8–5 and was, e.g., 0.04 units at pH 7.4. While ASICs are known to be gated by extracellular acidification, intracellular pH has been shown to modulate ASIC1a currents [53]. Intracellular acidification was shown to decrease peak current amplitudes and to accelerate open channel inactivation, however, with shallow pH dependence [53]. Because we used in our experiments HEPES to buffer the intracellular solutions, intracellular pH changes due to changes in temperature may contribute to the observed effects. To test whether the intracellular pH shift due to the change in temperature in HEPES containing pipette solutions contributes to the observed functional changes in ASIC currents, we replaced in control experiments the HEPES in the pipette solution by MOPS. Under these conditions, ASIC1a whole-cell currents inactivated with a Q10 of 2.25± 0.20 between 25°C and 35°C (pH 6.5, $n=5$), a value close to the Q10 measured with HEPES containing pipette solution (pH 6.7, 1.97±0.16, $n=7$).

Capsaicin and 4-(3-chloro-2-pyridinyl)-*N*-[4-(1,1-dimethylethyl)phenyl]-1-piperazinecarboxamide (BCTC) were added from stock solution in DMSO (final DMSO concentration 0.1%). Chemicals were obtained from Acros Organics (Geel, Belgium), Applichem (Darmstadt, Germany), Enzo Life Sciences (Lausen, Switzerland), Sigma, or Fluka (Buchs, Switzerland).

Temperature control

Temperature was controlled using a temperature control unit connected to the MPRE8 perfusion system (TC2Bip, Cell MicroControls, Norfolk, USA). Bath temperature was measured using a temperature probe (Th-10Km, Cell MicroControls, Norfolk, USA) and was found to be accurately controlled at the exit of the perfusion system (data not shown). Temperature ramps were controlled from the Patchmaster software. Unless mentioned, measurements were performed in steady-state temperature conditions.

Analysis and statistics

Current traces were fitted using the equation: $I = I_{min} + I_{max}*\exp(-t/\tau_I)$ where I_{min} and I_{max} are the minimum and maximal currents, t the time and τ_I the time constant of inactivation. The pH activation curves were fitted using the Hill equation: $I = I_{max}/\left[1 + \left(10^{-pH_{0.5}}/10^{-pH}\right)^{nH}\right]$, where I_{max} is the maximal current, $pH_{0.5}$ is the pH at which half of the maximal current is measured, and nH is the Hill coefficient. Steady-state inactivation curves were fitted by an analogous equation. Recovery from inactivation curves were fitted by using a monoexponential fit equation: $I = 1 - \exp^{-(t-d)/\tau_R}$, where I is the normalized current amplitude, τ_R is the exponential time constant and, d is the delay. Conductance–voltage activation curves were fitted using the following Boltzmann function: $G = (G_{max} - G_{min})/\left(1 + e^{-((zF)(V-V_{0.5})/RT)}\right) + G_{min}$ where G is the conductance, G_{min} and G_{max} are the minimal and maximal conductance, V is the voltage, $V_{0.5}$ is the voltage that elicits half-maximal conductance, z is the gating charge, F is the Faraday constant, and R is the gas constant. Data are presented as mean ± SEM. Differences between temperature conditions in comparisons where two values were compared at two temperatures were analyzed using Student's t test. Statistical differences between groups are indicated by asterisks: * ($p<0.05$), ** ($p<0.01$), and *** ($p<0.001$). Situations where more than two conditions exist at two temperatures were compared using two-way ANOVA. Statistical difference between groups are indicated by number signs: # ($p<0.05$), ## ($p<0.01$), and ### ($p<0.001$).

Results

ASIC open channel inactivation kinetics are accelerated at higher temperature

ASIC currents were recorded in the whole-cell patch clamp mode from CHO cells stably expressing ASIC1a, ASIC1b, ASIC2a, or ASIC3. Increasing the temperature from 25°C to 35°C accelerated open channel inactivation of all ASIC subtypes as illustrated in Fig. 1a, resulting in a shorter duration of the transient current. The temperature-induced changes in inactivation kinetics were fully reversible and did not depend on whether the experiment was started at 25°C or 35°C (data not shown). To quantify the kinetics, the inactivating part of the current traces was fitted to a single exponential (see "Materials and methods"), yielding the time constant of inactivation τ_I (Fig. 1b). Figure 1b also shows the Q10 index for the inactivation kinetics, which was calculated as the ratio of τ_I at 25°C/τ_I at 35°C. The Q10 value was low for ASIC3, intermediate for ASIC1a and ASIC1b, and greatest for ASIC2a (Fig. 1b). The Q10 values of ASIC1a, ASIC1b, and ASIC2a inactivation are close to or in the range of typical values for gating processes involving conformational changes of ion channels (≥2) [17]. Similar Q10 values were obtained over a wide range of test pH (data not shown). The

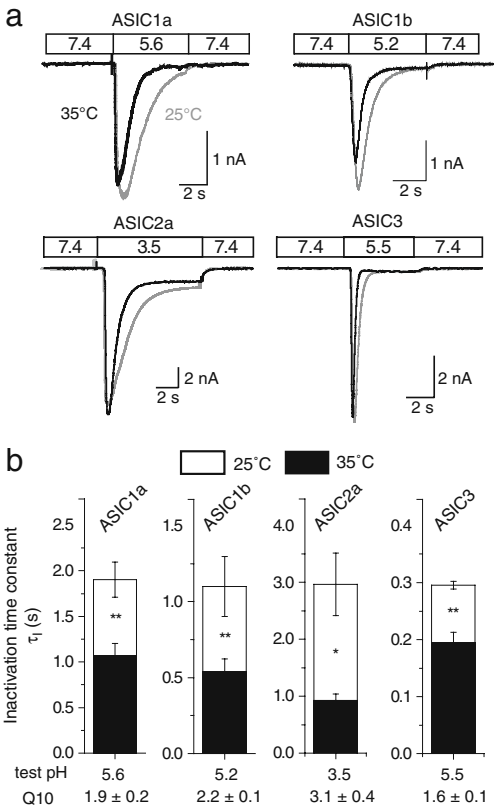

Fig. 1 Increasing the temperature accelerates ASIC open channel inactivation. ASIC homomultimers (ASIC1a, ASIC1b, ASIC2a, and ASIC3) stably expressed in CHO cells were activated by lowering the pH from a conditioning pH of 7.4 to the indicated acidic pH. Currents were measured in whole-cell patch clamp at a holding potential of −60 mV. **a** Typical ASIC current traces at 25°C (*gray*) and 35°C (*black*) for the indicated pH values are shown. **b** The time constant of open channel inactivation (τ_I, see "Materials and methods") is plotted for the given test pH values at 25°C (*open bars*) and 35°C (*filled bars*). Difference between temperatures assessed by Student's paired t test; n=5–7. Open channel inactivation Q10, the ratio of τ_I at 25°C and 35°C (τ_{I25}/τ_{I35}) is indicated

inactivation kinetics of ASIC3 are faster than those of the other ASICs (Fig. 1) and are in our experiments possibly limited in part by the speed of the solution change. The small Q10 values for ASIC3 open channel inactivation may therefore be due in part to this experimental limitation.

Inactivated ASICs require exposure to a sufficiently alkaline pH for a certain duration to leave the inactivated state and to be ready for activation by acidification. As a second measure of the kinetics of a transition between conformational states of the channel, we determined this time course of the recovery from inactivation. These experiments were done with ASIC1a, which has the slowest recovery time course among ASIC subtypes [2, 36] (Supplementary Fig. S1a, online resource 1). Recovery from inactivation was accelerated with increasing temperature, however, with a low Q10 value of 1.52±0.02 (Supplementary Fig. S1b and S1c, online resource 1), indicating low temperature dependence.

Temperature dependence of ASIC activation and steady-state inactivation

To characterize the pH dependence of activation of cloned ASICs, we performed step pH changes from pH 7.4 (7.6 for ASIC1a) to acidic solutions of different pH. For illustration, the protocol used for ASIC1b is shown on the left panel of Fig. 2a, and current traces obtained at the two temperatures are shown in the middle and right panels. Steady-state inactivation (SSIN) represents the transition from the closed to the inactivated state during prolonged exposure to moderately acidic pH. SSIN determines the fraction of channels that are available for opening at a given conditioning pH. A typical SSIN pH dependence protocol for ASIC2a is illustrated in Fig. 2b (left panel), and current traces obtained in a typical experiment with ASIC2a performed at 25°C and 35°C are shown in the middle and right panels. For each ASIC type, the normalized current of activation experiments is plotted as a function of the test pH, together with the normalized currents of the SSIN experiments that are plotted in Fig. 2c as a function of the conditioning pH. Individual experiments were fitted with the Hill equation (see "Materials and methods"), yielding the pH of half-maximal activation ($pH_{0.5}$), or the pH of half-maximal inactivation ($pHIn_{0.5}$) and the Hill number (*nH*), which are indicated in Table 1. As shown in Fig. 2c and in Table 1, the increase in temperature did not significantly affect the pH dependence of activation of ASIC1a, ASIC1b, ASIC2a, and ASIC3. In contrast, the increase in temperature shifted the inactivation curve of ASIC1a, ASIC1b, and ASIC2a to slightly more alkaline pH. As a consequence, if ASIC1a, ASIC1b, or ASIC2 is activated from a conditioning pH corresponding to the steep part of their SSIN curve, the currents are expected to be smaller at the higher temperature.

The ASIC-mediated charge transfer is reduced with increasing temperature

ASIC activation in neurons has been shown to induce action potentials [10, 35, 49]. The extent and the duration of the ASIC-mediated depolarization depend not only on the amplitude of the ASIC activity but also on the number of charges the channels transport during their opening. We tested therefore whether either of these parameters, the peak current amplitude and the number of transported charges during channel opening (termed here "charge transfer"), were affected by a change in temperature. Figure 3a shows the normalized peak current density measured at a saturating pH for the two temperatures 25°C and 35°C for each ASIC subtype. ASIC1a and ASIC1b showed a reduction in peak current density at 35°C. ASIC2a presented a modest increase in peak current density at 35°C while no modifications were observed with ASIC3. The observed shift in $pHIn_{0.5}$ may contribute to the ASIC1a current decrease at the higher temperature because it is expected to lead to partial inactivation of ASIC1a at the conditioning pH of 7.4 (Fig. 2c). For other ASIC types, such a contribution is not possible because the steep part of their SSIN curve occurs at pH values that are more acidic than the conditioning pH (7.4; Fig. 2c). The charge transfer was calculated by integrating the area under the current trace from activation to complete open channel inactivation during a 10-s acidification. Figure 3b presents the ratio of the charge transfer at 35°C/ charge transfer at 25°C. As expected from the lower peak inward current density and faster open channel inactivation kinetics at the higher temperature, increasing the temperature from 25°C to 35°C resulted for all ASIC subtypes in an approximately two-fold reduction in charge transfer during a 10-s acidification.

While ASIC1a and ASIC1b currents rapidly decrease to the baseline during an acidic stimulation, ASIC2a and ASIC3 display a small sustained current at the end of a 10-s stimulation (Fig. 1a). This sustained current appears mainly in the more acidic pH range [27, 40, 51, 52]. Figure 3c presents the sustained current fraction calculated as the ratio of the sustained current and the peak current, in percent. The ASIC2a sustained current fraction was reduced by about 30% by the temperature increase from 25°C to 35°C while the ASIC3 sustained current fraction was temperature independent. The decrease of the sustained ASIC2a current at 35°C is likely due to a decrease in the relative energy of the inactivated versus the open state at this temperature. Taken together, the current densities of ASIC1a and ASIC1b, the number of transported charges of all ASICs, and the amplitude of the sustained ASIC2a current are reduced at 35 relative to 25°C.

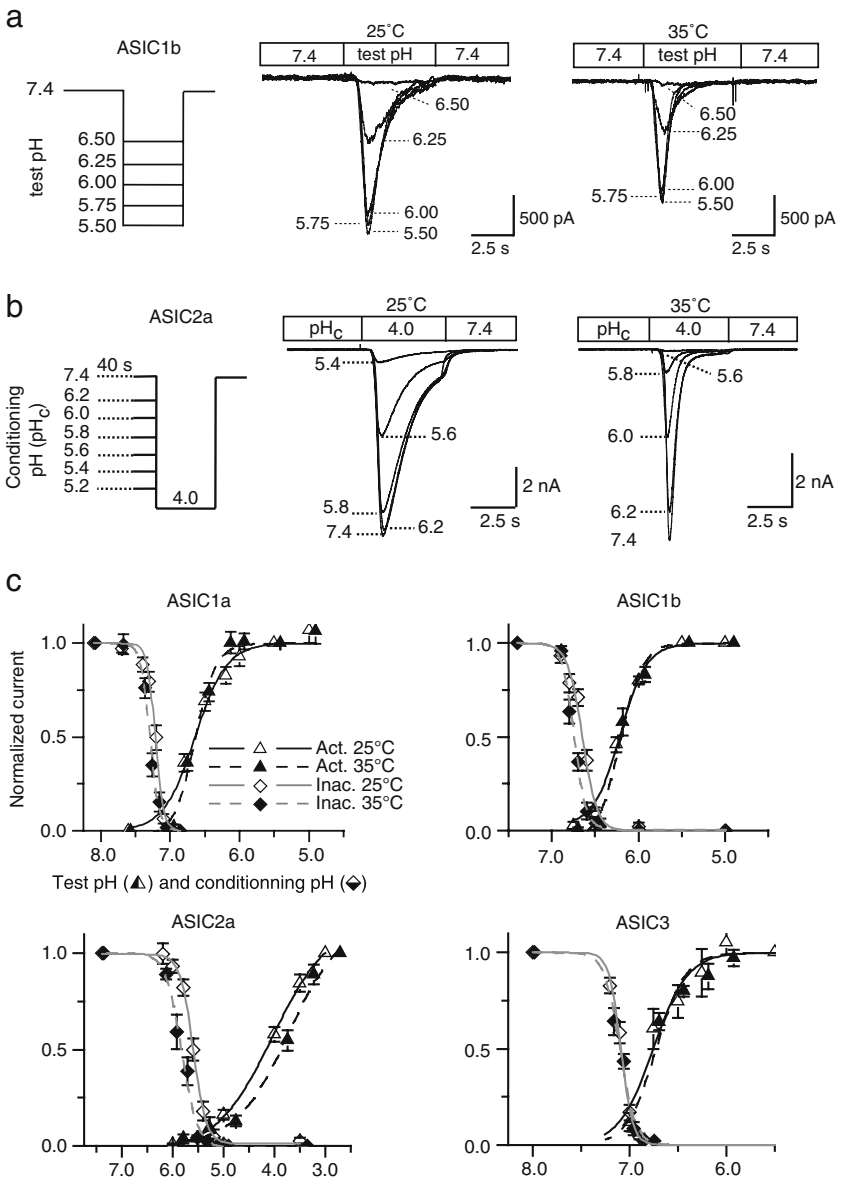

Fig. 2 ASIC pH dependence of steady-state inactivation is temperature dependent. The currents were measured from CHO cells stably expressing the ASIC subunits, in whole-cell voltage clamp to −60 mV. **a** A typical ASIC1b activation curve protocol (*left*) and traces at 25°C (*middle*) and 35°C (*right*) are shown. ASICs were activated by lowering the pH from 7.4 (7.6 for ASIC1a) to the indicated pH values for 5 s, followed by 30- to 60-s recovery at pH 7.4. **b** A conditioning pH in the range of 8–5, depending on the ASIC subtype tested, was applied for 40 s and the fraction of non-inactivated channels was measured by applying an acidic pH. This protocol was repeated with increasingly acidic conditioning pH until no current remained during the acidic stimulus, as illustrated in the *left panel*. Typical ASIC2a traces obtained from two different cells at 25°C (*middle*) and 35°C (*right*) are shown. Note that due to the short duration of the test pulses inactivation did not reach a steady state at 25°C at the end of the test pulse. **c** Normalized activation and steady-state inactivation (SSIN) curves are plotted as a function of the test pH of activation at 25°C (*empty triangle*) and 35°C (*filled triangle*) or conditioning pH of SSIN at 25°C (*empty diamond*) and 35°C (*filled diamond*). *Solid and interrupted lines* represent the fit to the Hill equation (see "Materials and methods") at 25°C and 35°C for activation (*black*) and steady-state inactivation (*gray*), respectively. The fit parameters are shown in Table 1, (n=5–7)

The amplitude of H^+-gated currents of cloned TRPV1 increases with temperature

The effect of temperature on TRPV1 was assessed by whole-cell patch clamp on CHO cells stably expressing TRPV1. Figure 4a shows a typical trace of TRPV1 current induced by a heat ramp from 25°C to 50°C at pH 7.4. The average current response measured in such experiments is plotted in Fig. 4b for heat ramps at pH 7.4 and 6.5. Ten percent of the maximal heat-induced current was reached at 40.2±1.2°C when carried out at pH 7.4 (n=11) and at 36.4±1.5°C when done at pH 6.5 (n=10), indicating that

Table 1 pH dependence of cloned ASICs and TRPV1 at 25°C and 35°C

		ASIC1a	ASIC1b	ASIC2a	ASIC3	TRPV1
Activation, $pH_{0.5}$	25°C	6.63±0.06	6.22±0.05	4.03±0.06	6.73±0.07	5.31±0.10
	35°C	6.66±0.03	6.18±0.07	3.83±0.08	6.66±0.03	5.38±0.10
Steady-state inactivation, $pHIn_{0.5}$	25°C	7.20±0.02	6.65±0.01	5.58±0.03	7.10±0.02	–
	35°C	7.29±0.02**	6.69±0.01*	5.78±0.05**	7.08±0.02	–

The pH of half-maximal activation ($pH_{0.5}$) and pH of half-maximal inactivation ($pHIn_{0.5}$) were obtained by fitting the experimental data to the Hill equation, as described in the text and under "Materials and methods"

–, not determined

*$p<0.05$; **$p<0.01$, different from the corresponding parameter obtained at 25°C (*t* test), $n=4–7$

acidification shifts the temperature dependence to lower values, consistent with previous studies [42]. In TRPV1-expressing cells, the average heat-evoked current density at 50°C was −171±46 pA/pF at pH 6.5 ($n=10$) and −96±33 pA/pF at pH 7.4 ($n=9$). The heat-evoked current density in non-transfected cells was negligible with −12±10 pA/pF at pH 6.5 ($n=3$) and −7±6 pA/pF at pH 7.4 ($n=3$). The analysis of the heat-evoked TRPV1 currents with Arrhenius plots is illustrated in Supplementary Fig. S2 (online resource 2) and yielded Q10 values in the steep phase of 12.0±2.0 ($n=8$) at pH 7.4 and of 8.8±0.8 at pH 6.5 ($n=10$). The relatively low Q10 values are likely due to the absence of external Ca^{2+} in these experiments [50]. The threshold temperature as determined from the Arrhenius plot analysis was 41±1°C at pH 7.4 ($n=8$). At pH 6.5, the threshold was not in all experiments clearly detectable from the Arrhenius plot, due to a high-temperature dependence already at low temperatures.

The pH dependence of TRPV1 activation was determined in an analogous way as for ASICs, and typical current traces at 25°C and 35°C are presented in Fig. 4c. These traces also illustrate that channel opening is faster at the higher temperature. To quantify the current activation kinetics, the time constant of opening τ_O was determined by fitting the opening time course to a single exponential. At pH 6 and 5, a single exponential fitted the activation phase well. Figure 4d plots the time constant of activation measured at pH 6 and 5 at both temperatures, confirming the temperature dependence of TRPV1 activation kinetics. Comparison of the pH dependence of activation at the two temperatures (Fig. 4e and Table 1) indicates that the TRPV1 $pH_{0.5}$ does not change with temperature in the 25–35°C range. Figure 4f plots TRPV1 current amplitudes induced by acidification to pH 6, 5, and 4 at both 25°C and 35°C, measured in direct comparison. The higher temperature led to an increase in the current amplitudes induced over the pH range 6–4 that was 1.37–1.95-fold ($n=8–10$), dependent on the test pH. To test whether the temperature affected the voltage dependence of the pH 6-induced TRPV1 currents, we performed current–voltage protocols at the two temperatures. These experiments were carried out in TRPV1-transfected HEK cells because the CHO cells did not tolerate well the required voltage protocols. The general properties of H^+-induced TRPV1 currents were not different between TRPV1-expressing CHO and HEK cells (data not shown). In the presence of extracellular pH 6 solution, the cells were subjected to a series of 100-ms voltage steps from −100 to +220 mV in 20-mV increments from a holding potential of −60 mV (at 25°C and 35°C). Figure 4g illustrates the current response from a typical experiment, illustrating the large outward currents at positive voltages. Conductance–voltage relationships were constructed and fitted with a Boltzmann function (see "Materials and methods") yielding the voltage of half-maximal conductance ($V_{0.5}$) and maximal conductance G_{max}. $V_{0.5}$ was 87±14 and 52±14 mV at 25°C and 35°C, respectively (Fig. 4h, solid (25°C) and dashed (35°C) line), yielding a hyperpolarizing shift of −35±9 mV when the temperature was increased from 25°C to 35°C ($n=6$). The outward conductance at +220 mV was 1.44±0.11 ($n=5$)-fold larger at 35 as compared to 25°C (Fig. 4h). This analysis also showed a significant increase in conductance at −60 mV when the temperature was raised from 25°C to 35°C (Fig. 4h, inset).

ASIC temperature dependence is similar in rat DRG neurons as in the recombinant expression system

Because increasing the temperature accelerated the open channel inactivation, thereby reducing the charge transfer of cloned ASICs, we were interested in determining the effect of a temperature increase in a physiological model of pH sensing. Small diameter neurons of rat DRGs are known to express TRPV1 and all ASICs. In a previous study from our laboratory, three types of endogenous ASIC-mediated currents were found in small diameter DRG neurons [35]. Type 1 currents showed slow open channel inactivation kinetics ($\tau_I>0.5$ s at pH 6) and a ratio of pH 4-induced current amplitude/pH 6-induced current amplitude ($I_{pH\ 4}/I_{pH\ 6}$) of around 1. These properties

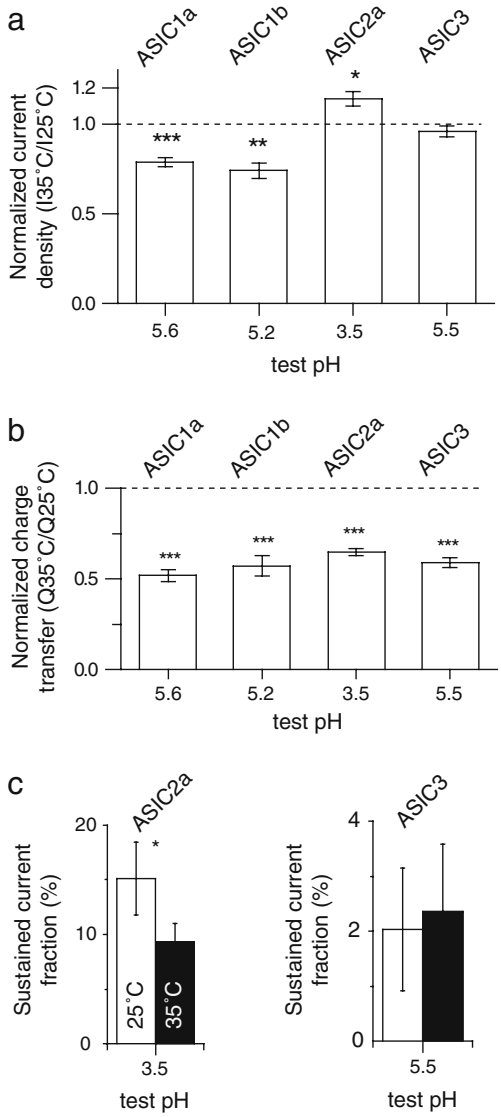

Fig. 3 Temperature dependence of ASIC peak current amplitudes and charge transfer. **a** The ratio of peak inward current density obtained at 35°C and 25°C is plotted for the given saturating test pH for the different ASIC subtypes, n=5–7. *Asterisks* indicate statistical difference from 1, assessed by one sample t test. **b** Ratio of charge transfer density (measured as the integral of the current, normalized to the cell capacitance) at 35°C to that at 25°C at given saturating test pH for the different ASIC subtypes, n=4–6. One sample t test. **c** The sustained current fraction (in percent) was obtained by taking the ratio of the sustained current at the end of a 10-s acidification to the peak current at 25°C and 35°C. Results are shown for ASIC2a and ASIC3, paired t test, n=4–6

combined with complete inhibition by the ASIC1a-specific tarantula toxin Psalmotoxin 1 [13] had identified type 1 current as carried by homomultimeric ASIC1a channels [35]. Type 2 and 3 current types are fast inactivating populations of channels (τ_I<0.5 s) with $I_{pH\ 4}/I_{pH\ 6}$ ratio >2 and <2, respectively. These currents are thought to be composed of heteromultimeric populations of ASIC1, ASIC2, and ASIC3 channels [35]. The kinetics and pH dependence, as well as the absence of a sustained current, suggest that type 3 current is mediated by channels containing ASIC3 and ASIC1a/1b together with likely a third subunit, since dual subunit combinations do not reproduce this current type [8, 16]. ASIC type 2 currents were found in 15% of small diameter DRG neurons by Poirot and colleagues and were not analyzed in the present study because they represent only a small fraction of ASIC currents in DRG neurons and because they require more acidic pH for activation (biphasic activation with major $pH_{0.5}$=~5) than the other two ASIC current types. Figure 5a presents typical traces of type 1 and type 3 ASIC current types at 25°C and 35°C in neurons that had no measurable TRPV1 current at this pH. Open channel inactivation kinetics were accelerated for both current types when the temperature was raised from 25°C to 35°C (Fig. 5b), with Q10 values of ~2.5 for type 1 currents and of ~1.5 for type 3 currents. The $pH_{0.5}$ of the type 1 current was slightly shifted to more acidic values at 35°C, while the type 3 current $pH_{0.5}$ was temperature independent (Fig. 5c, Table 2). The type 1 ASIC currents of rat DRG neurons had a more alkaline $pH_{0.5}$ than the cloned mouse ASIC1a (6.37±0.04 vs. 6.66±0.03 at 35°C, Tables 1 and 2). Since the mouse and rat ASIC1a protein sequences differ only in one residue, it is likely that the observed difference is due to different interacting proteins and/or regulation in the two cell types. Type 1 and 3 current amplitudes were reduced with increasing temperature (Fig. 5d). This temperature-dependent decrease was stronger than observed in the cloned ASIC channels. At least in part, this difference is likely due to the fact that the $pHIn_{0.5}$ of the type 1 and type 3 currents is close to 7.3 [35]. A further alkaline shift of $pHIn_{0.5}$ by the increase in temperature to 35°C will likely lead to partial SSIN of ASICs at the conditioning pH of these experiments, pH 7.4.

In summary, the ASIC current types 1 and 3 of DRG neurons showed a similar temperature dependence of the kinetics and the pH dependence of activation as the cloned ASICs expressed in CHO cells while the temperature dependence of peak current amplitudes was stronger in DRG neurons.

Temperature dependence of the endogenous rat DRG TRPV1 channel

The ability of the endogenous DRG TRPV1 channel to be opened by heat was first tested by performing a 30-s 25–50°C heat ramp at either pH 7.4 or 6.5 (Fig. 6a). Acidification to pH 6.5 increased the heat-evoked current amplitude (not shown) and shifted the heat activation threshold to lower temperatures (Fig. 6b). At pH 7.4, 10% of the maximal heat-invoked inward current amplitude was reached at 40.9±1.3°C (n=9) while at pH 6.5, 10% of the maximal current was reached at 36±1.8°C (n=10). Anal-

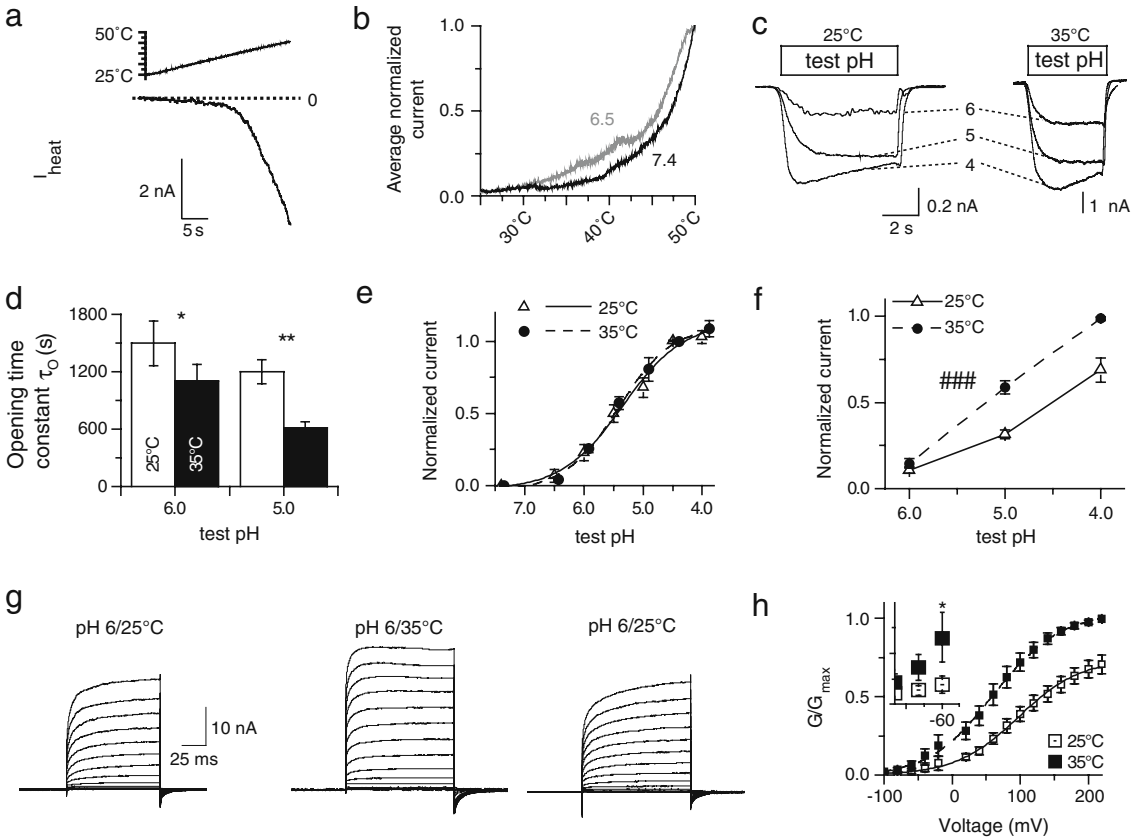

Fig. 4 Proton-induced currents of cloned TRPV1 are temperature dependent. TRPV1 currents were measured from CHO cells stably expressing TRPV1 (and from transiently transfected HEK cells for the voltage dependence), in whole-cell voltage clamp to −60 mV in Ca^{++}-free solutions. **a** The *diagram on the upper part* illustrates the heat ramp used for the measurement of the TRPV1 heat-activated currents. A typical heat-evoked current trace obtained at Ph 7.4 is shown in the *bottom*. Perfusion temperature was increased linearly from 25°C to 50°C in 30 s. **b** The average, normalized heat-evoked response obtained is plotted as a function of the perfusion temperature, measured at pH 7.4 or pH 6.5 (n=10–11). *Error bars* are small and omitted for clarity. **c** Cells expressing TRPV1 were activated by a pH drop from 7.4 to the indicated test pH. Typical traces (obtained from two different cells) at 25°C (*left*) and 35°C (*right*) are shown. **d** The time constant of opening (τ_O) values are plotted with respect to the stimulation pH at 25°C (*open bars*) and 35°C (*filled bars*), obtained by fitting a single exponential to the opening phase of the current trace. *p<0.05, τ_O depends on temperature, paired t test, n=5–20. **e** Current amplitudes, normalized to the value measured at the most acidic test pH, are plotted as a function of the stimulation pH at 25°C (*empty triangle*) and 35°C (*filled circle*). *Solid and interrupted lines* represent the fit to the Hill equation at 25°C and 35°C, respectively (n=6–7). The $pH_{0.5}$ values of the fits are indicated in Table 1. **f** Current amplitudes for acidification to pH 6, 5, and 4 at 25°C (*open bars*) and 35°C (*filled bars*) were measured in direct comparison and normalized to the response to pH 4 at 35°C (###p<0.001, two-way ANOVA, n=7–9). **g** HEK cells expressing TRPV1 were voltage-clamped to −60 mV and subjected to a protocol of 100-ms voltage steps between −100 and +220 mV in 20 mV increments at 25°C or 35°C in pH 6 solutions. The pH 6 solution was applied 10 s prior to the recording of the *I–V* curve to completely inactivate the endogenous ASIC1a currents. A typical experiment is shown. **h** Conductance was normalized to the highest value measured at 35°C for a given cell and plotted as a function of voltage. A Boltzmann function was used to fit the conductance–voltage curve (*solid* and *dashed lines*). Direct comparison of $V_{0.5}$ at 25°C and 35°C gave a hyperpolarizing $V_{0.5}$ shift (*p<0.05, paired t test). The conductance was larger at 35°C compared to 25°C (n=5). The conductance at −60 mV was different between 25°C and 35°C (*p< 0.05, paired t test, n=6; **h** *inset*)

ysis of the heat-evoked current by Arrhenius plots yielded Q10 values of the steep phase of 14.9±1.3 at pH 7.4 and 8.3±1.0 at pH 6.5 (n=7–10). The activation threshold determined from Arrhenius plots at pH 7.4 was 41±1°C. The current induced by a 30-s heat ramp was reversibly inhibited by 94±4% (n=4) in DRG neurons by a 60-s preincubation with 100 nM BCTC, a TRPV1 inhibitor that binds to the capsaicin binding site (Fig. 6c) [45]. Together with the activation threshold of this current and its modulation by pH (see below), this strongly suggests that the current induced by the heat ramp is mainly carried by TRPV1. Typical H^+-induced TRPV1 current traces are shown in Fig. 6d. The traces indicate that the current amplitude increased with increasing temperature. Figure 6e shows that the temperature increase led to a 1.6–2.4-fold increase in peak current density, depending on the test pH. The pH dependence of activation of H^+-gated currents measured at 25°C and 35°C was, however, temperature independent (Fig. 6f), consistent with the behavior of the cloned TRPV1 channel (Fig. 4). These experiments thus

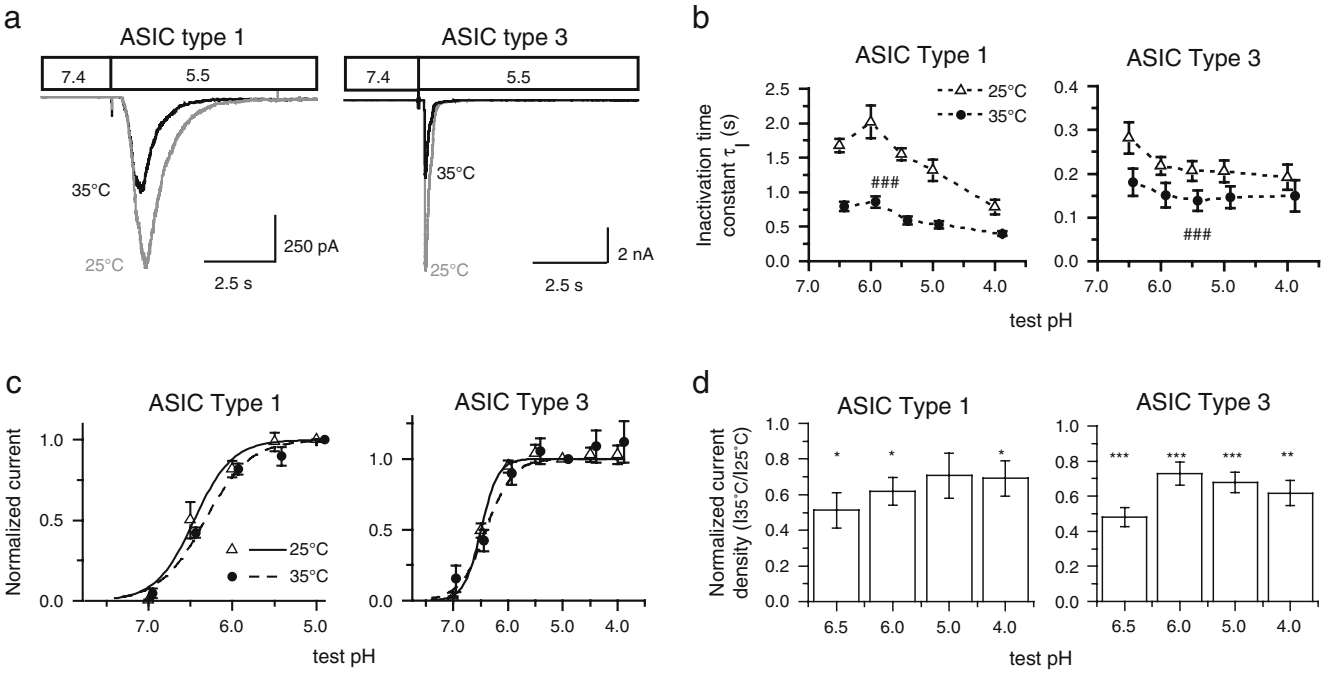

Fig. 5 Temperature accelerates open channel inactivation kinetics and reduces peak inward current amplitudes of DRG ASIC currents. Endogenous type 1 and 3 ASIC currents of DRG neurons were measured in whole-cell voltage clamp to −60 mV. **a** Typical ASIC type 1 and 3 current traces are shown for pH 5.5 stimulation at 25°C (gray) and 35°C (*black*). These traces were measured from neurons which did not express TRPV1 currents. **b** The time constant of open channel inactivation (τ_I), obtained by fitting a single exponential to the inactivating phase of the current trace (see "Materials and methods"), is plotted as a function of the stimulation pH at 25°C (*empty triangle*) and 35°C (*filled circle*), n=5–13. ###p<0.001, τ_I values are different between 25°C and 35°C, two-way ANOVA. **c** Normalized currents are plotted as a function of the stimulation pH at 25°C (*empty triangle*) and 35°C (*filled circle*). *Solid and interrupted lines* represent the fit to the Hill equation at 25°C and 35°C, respectively, and the obtained $pH_{0.5}$ values are indicated in Table 2, n=7–14. **d** ASIC peak current induced by pH 6.5, 6, 5, and 4 at 35°C normalized to current at 25°C, shown for type 1 and type 3 currents (*left* and *right*, respectively). Paired t test, n=4–16

show that the endogenous rat TRPV1 is efficiently activated by high temperature, that the temperature dependence is shifted to lower temperatures by simultaneous acidification, and that H^+-gated currents are increased between 25°C and 35°C without a shift in the pH dependence of activation.

The relative contribution of ASICs and TRPV1 to H^+-gated currents depends on temperature

We measured the amplitudes of the acid-induced transient ASIC and sustained TRPV1 currents in small diameter DRG neurons at physiological ion concentrations in the extracellular solution. Co-expression of ASIC and TRPV1 is frequently found in small diameter DRG neurons. However, due to their different pH dependence and kinetics and the previous observation that ASIC type 1 and 3 currents of small diameter DRG neurons have practically no sustained component [35], these currents can be separated for the analysis. Figure 7a shows typical acid-induced currents from a DRG neuron co-expressing ASIC type 3 and TRPV1 currents at 25°C and 35°C. As described previously in this study for cloned and endogenous ASICs, the transient current amplitude, which is mediated by ASICs, was decreased when the temperature was raised from 25°C to 35°C (Figs. 3a and 5d). The amplitude of the sustained current, which is mostly mediated by TRPV1, was slightly increased at 35°C (Fig. 7a). Figure 7b illustrates an experiment from a neuron expressing similar ASIC and TRPV1 currents as in Fig. 7a and shows the current response at 25°C to different acidic pH values in the range of 6 to 4. While the transient current amplitude had reached its maximum at pH 6, the amplitude of the sustained current, mediated mostly by TRPV1, increased strongly in the pH range of 6 to 4 (Fig. 7b). To confirm that

Table 2 Activation pH dependence of DRG ASICs and TRPV1 at 25°C and 35°C

		ASIC type 1	ASIC type 3	TRPV1
$pH_{0.5}$	25°C	6.47±0.09	6.48±0.04	5.13±0.12
	35°C	6.37±0.04**	6.40±0.06	5.09±0.04

The pH of half-maximal activation ($pH_{0.5}$) was obtained by fitting the data to the Hill equation ("Materials and methods")

**p<0.01, different from the corresponding parameter obtained at 25°C (t test), n=4–8

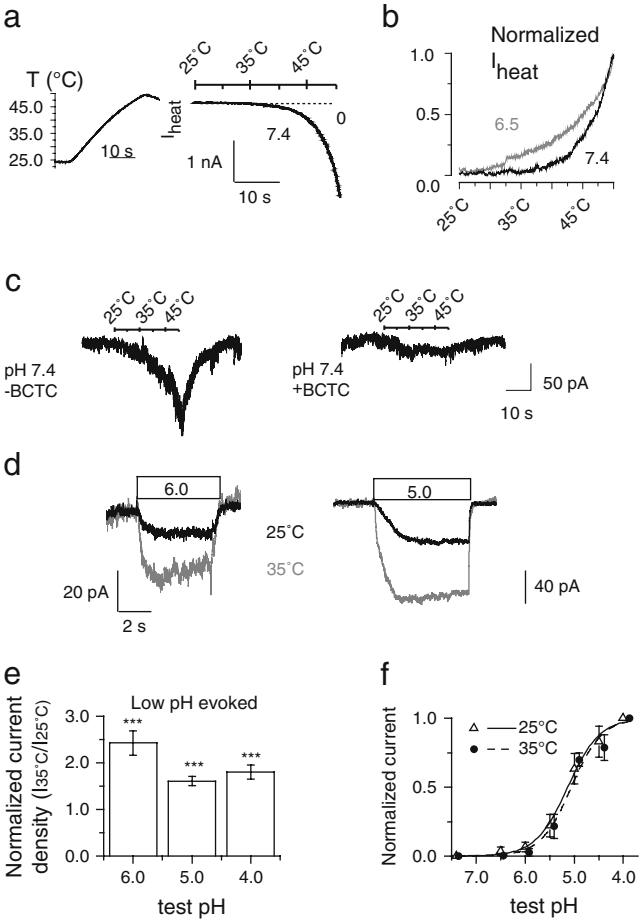

Fig. 6 Characterization of temperature- and H^+-induced TRPV1 currents in DRG neurons. Currents were measured from small diameter DRG neurons in whole-cell voltage clamp to −60 mV in Ca^{++}-free solutions. **a** Illustration of the heat ramp applied to DRG neurons (*left panel*). *Right panel*, a typical heat ramp response at pH 7.4 is shown. **b** Average heat-induced current at pH 6.5 or 7.4 (n=7–8). *Error bars* are small and omitted for clarity. **c** Traces from a representative heat ramp experiment carried out with (*right*) or without (*left*) a 60-s preincubation with 100 nM BCTC. **d** Typical traces from a DRG neuron expressing TRPV1 are shown for pH 6 and 5 at 25°C and 35°C (*black* and *gray*, respectively). **e** Acid-induced TRPV1 current amplitudes measured at 35°C were normalized to the value obtained at 25°C and are shown for three different values of stimulation pH. Paired t test (n=12–22). **f** Activation curves of TRPV1 current in DRG neurons, measured from a conditioning pH of 7.4. Normalized currents obtained at 25°C (*empty triangle*) and 35°C (*filled circle*) are plotted. *Solid and interrupted lines* represent the fit to the Hill equation at 25°C and 35°C, respectively, and $pH_{0.5}$ values are shown in Table 2, n=6–7

the transient current is mediated by ASICs, we applied in a separate set of experiments a conditioning pH of 7.0 during 40 s prior to the ASIC activation by pH 6 and compared the pH 6-induced transient current amplitude to that obtained in the same cell with a conditioning pH of 7.4. The conditioning exposure to pH 7 is expected to inactivate ASIC currents (Fig. 2c) [35]. This method of separation yielded the TRPV1-mediated sustained component with no measurable transient component, confirming the transient component as ASIC current (Fig. 7c, representative traces on the left, summarized on the right). Control experiments with cloned TRPV1 showed that a 40-s exposure to pH 7.0 did not inhibit TRPV1 currents (I_{TRPV1} after 40-s conditioning at pH 7.0=98±9% of I_{TRPV1} after control conditioning at pH 7.4, n=6). To test for the presence of TRPV1 in neurons expressing a sustained acid-induced current, we measured the capsaicin-induced current in such neurons in a set of experiments. In all neurons tested with a detectable (i.e., >10 pA) pH 6-induced sustained current, 1 μM capsaicin induced a current (current density=−134±30 pA/pF, 25°C, n=9). The sustained current induced by pH 4, pH 5, or capsaicin was reversibly inhibited by ~90% by the TRPV1 antagonist BCTC at 100 nM (Fig. 7d) [45]. These observations, in addition to the specific pH dependence and the slow activation kinetics, are consistent with TRPV1 mediating the sustained acid-induced current. Figure 7e plots the ratio of the TRPV1 current amplitude (measured at the end of a 10-s acidification)/ASIC current amplitude (measured as the transient component) at pH 6, 5, and 4 at 25°C and 35°C. This analysis indicates that the current amplitude induced by pH 6 was higher for ASICs at both temperatures. As expected from their pH dependence, the ratio between the current amplitude of TRPV1 and ASICs increases with acidic pH and temperature (Fig. 7e). DRG neurons are a very heterogeneous population of cells, with variable ASIC and TRPV1 current expression levels, reflected by the large error bars of the ASIC/TRPV1 current ratio (Fig. 7e). To evaluate the contribution to the sustained activity, we have determined the charge transfer, as the integral of a 1-s segment of trace at the beginning (ASIC) and at the end (TRPV1) of an acidic pulse [32]. This analysis is shown in Fig. 7f and suggests that during a 1-s period of the stimulation, the ratio of charge transfer by TRPV1 relative to ASIC increases with temperature and acidic pH. Due to the high cell-to-cell variability in channel expression levels, the increase from 25°C to 35°C induced only a significant change in charge transfer ratio at pH 6.

Neuronal ASIC-mediated excitability is modulated by temperature

To determine whether there are differences in acid-induced neuronal activity between 25°C and 35°C, we activated ASICs by extracellular acidification from 7.4 to moderately acidic pH values (≥pH 6) in small diameter DRG neurons under current clamp and measured the amplitude of the depolarization and the number of induced action potentials (APs; Fig. 8). The change in membrane potential induced by pH 6.8 has two components, a slow depolarization to about −30 mV that takes about a second to reach its maximum and then decays slowly at 25°C and faster at

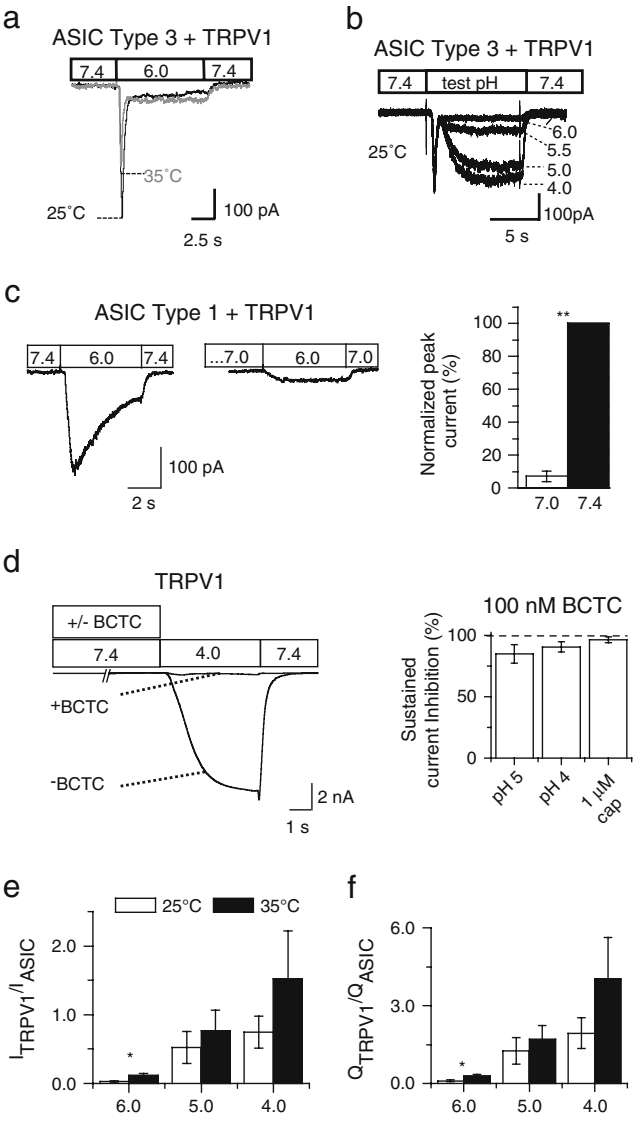

Fig. 7 Distinct temperature dependence of ASIC and TRPV1 currents in DRG neurons. All currents were measured from small diameter DRG neurons in whole-cell voltage clamp to −60 mV. **a** Typical pH 6-evoked currents recorded from a neuron co-expressing type 3 ASIC current and TRPV1 current, at 25°C (*black*) and 35°C (*gray*). **b** Typical current traces from a neuron expressing type 3 ASIC current and TRPV1 current, induced by acidification to the pH values indicated, at 25°C. **c** Neurons expressing transient currents in response to a pH drop from 7.4 to 6 were exposed to pH 7 for 40 s in order to inactivate ASICs. Typical traces obtained from a neuron co-expressing ASIC type 1 and TRPV1 (confirmed with capsaicin) are shown, with preincubation at pH 7.4 (*left*) or 7.0 (*center*). *Right*, pH 6-induced current amplitude obtained under the two conditions, normalized to the response with conditioning at pH 7.4, $^{**}p<0.01$, paired *t* test, $n=12$. **d** Typical pH 4-evoked current trace from a DRG neuron expressing TRPV1 with or without a 60-s preincubation with 100 nM BCTC. The *right panel* shows the BCTC inhibition for pH 5 and 4 and 1 μM capsaicin stimuli. **e** Ratio of the TRPV1 current amplitude measured at the end of a 10-s acidification to pH 6/the ASIC peak current amplitude at the same pH, plotted for 25°C (*open bars*) and 35°C (*filled bars*). **f** The charge transfer was determined as the integral of the current over a 1-s period at the start of the 10-s acidification pulse (ASIC) or at its end (TRPV1). The TRPV1/ASIC charge transfer ratio is plotted for pH 6, 5, and 4 at 25°C (*open bars*) and 35°C (*filled bars*). Averaged data are presented as mean ± SEM. $p<0.05$, temperature dependent, unpaired *t* test, $n=7–11$

35°C. On top of this slow activity, a burst of action potentials is visible. The first, slow component reflects the H^+-induced depolarization, which is at the pH of 6.8 entirely mediated by ASICs due to the different pH dependence of TRPV1. To confirm that the observed slow depolarization is due to ASICs, we conditioned in a separate set of experiments neurons that expressed either type 1 or type 3 currents with pH 7, which inactivates ASICs (Fig. 7c), but does not affect the TRPV1 component. Conditioning by pH 7 reversibly reduced the pH 6-induced depolarization amplitude at 500 ms by 81±6% ($n=7$) of its value measured at pH 7.4 (data not shown). The observed acceleration of the decay of this component with higher temperature (Fig. 8a) reflects the accelerated open channel inactivation time course of ASIC currents observed at 35°C. In the experiments shown in Fig. 8a, the ASIC-mediated depolarization reached the activation threshold of voltage-gated Na^+ channels, inducing the firing of action potentials. Acidification induced in most neurons with a type 1 ASIC current one or more APs. Figure 8b illustrates how in most cells a TRPV1-mediated depolarization (corresponding to the slowly developing depolarization after the initial peak) developed after the ASIC-mediated depolarization. Such slow depolarization occurred only at pH≤6. The depolarization amplitude ΔV_m induced by a pH drop to pH≤6.5 showed a tendency to lower values for both channel types at 35°C (Fig. 8c), a difference that was, however, only statistically significant for type 3 currents. In neurons expressing type 1 ASIC currents, acidification led generally to a higher number of APs than in those expressing type 3 ASIC currents (Fig. 8d), likely due to the slower kinetics of the type 1 ASIC current. The number of APs was not significantly different between the two temperatures for either current type (Fig. 8d).

Taken together, we show in the current clamp experiments that acidification to pH values that mainly activate ASICs and less TRPV1 depolarizes neurons and induces APs. The amplitude of the depolarization has a pH dependence close to that of ASIC currents.

Discussion

In this study, we have characterized acid-evoked ASIC and TRPV1 currents at room and physiological temperature in a recombinant expression system and in small diameter DRG neurons where both channel classes are endogenously expressed. Although the pH dependence of TRPV1 was not modulated by temperature and that of

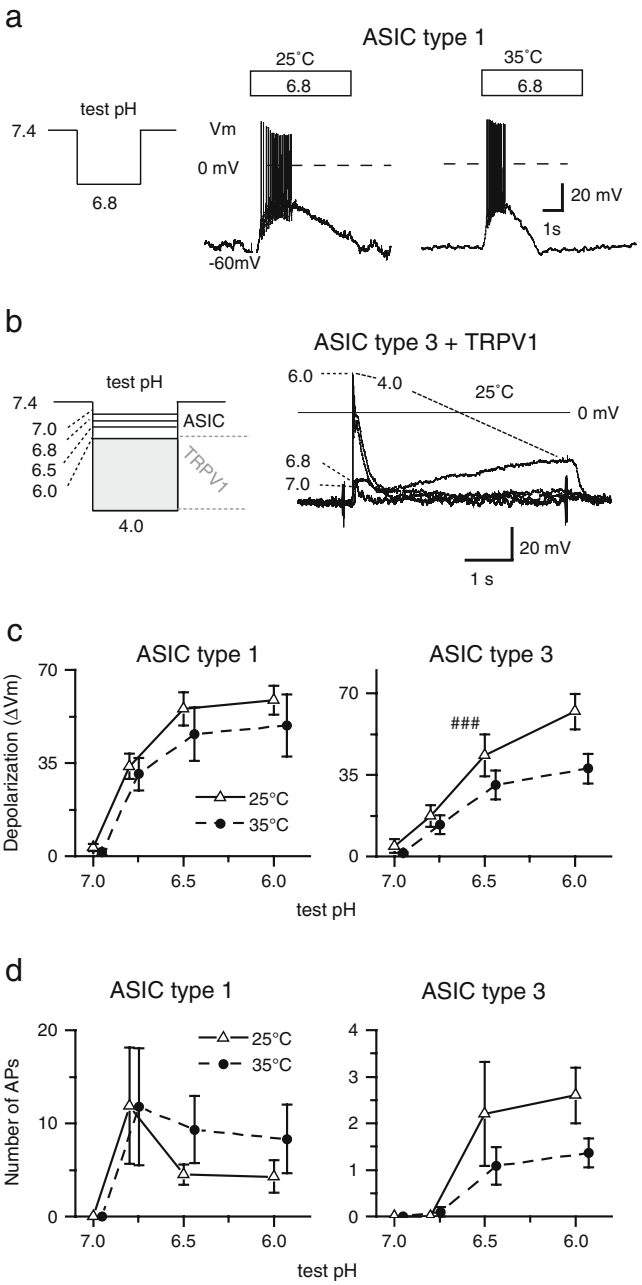

Fig. 8 Temperature modulates the acidification-induced depolarization of DRG neurons. Experiments were carried out in small diameter DRG neurons under current clamp. **a** The action potential (AP) induction protocol is shown on the *left*, and typical responses to an acidification to pH 6.8 are shown for the temperature of 25°C (*middle*) and 35°C (*right*). **b** Typical traces of acid-evoked depolarization obtained at 25°C from a neuron expressing ASIC type 3 current and TRPV1 current, with the protocol shown on the *left*. **c** The amplitude of the acidification-induced depolarization is plotted as a function of the stimulation pH at 25°C (*empty triangle*, *solid line*) and 35°C (*filled circle*, *interrupted line*), for neurons expressing type 1 or type 3 ASIC currents. The depolarization amplitude (ΔV_m) was determined as the difference in the membrane potential before the stimulation, and the peak of the smooth part of the acid-induced depolarization, i.e., the V_m between APs, n=5–10. **d** The number of induced APs during a 5-s acidification is plotted as a function of the stimulating pH at 25°C (*empty triangle*, *solid line*) and 35°C (*filled circle*, *interrupted line*) for neurons expressing type 1 or type 3 ASIC currents, n=5–12. ###$p<$ 0.001, different between 25°C and 35°C, two-way ANOVA

ASICs only to a small extent, we observed a reduction of ASIC and an increase of TRPV1 current amplitudes at 35°C and changes in current kinetics. This opposite temperature dependence of TRPV1 and ASICs increased the relative contribution of TRPV1 to pH sensing in DRG neurons at higher temperature.

Temperature dependence of ASICs

The increase in temperature to 35°C did not affect the ASIC activation pH dependence and induced small alkaline shifts in the inactivation pH dependence. This indicates that the difference in the energy of the three conformational states—closed, open, and inactivated—does not change completely with temperature in the temperature range between 25°C and 35°C, but that the increase in temperature favors to a certain extent the inactivated state. The most striking effect of the increased temperature was the reversible acceleration of open channel inactivation. This effect had previously been shown for some ASIC subtypes in a study that investigated ASIC kinetics in the temperature range of 6°C to 34°C [1] and recently for ASIC currents in DRG neurons [32]. A decrease in peak current amplitude with increasing temperature as observed in our study has previously been shown for cloned ASICs and some ASIC current types in sensory neurons [1, 32]. In contrast to these findings, ASIC-mediated currents were shown to be completely abolished upon increasing the temperature to 36°C in rat pulmonary sensory neurons [33]. This observation might be due either to a completely different environment in these neurons or to a differential regulation because Ni and Lee [33] used perforated patch recordings. Alternatively, it might be due to the fact that the highly thermally sensitive buffer HEPES was used in the extracellular solution [33], and therefore, the pH of the conditioning solution was lowered by the temperature increase, leading most likely to ASIC inactivation due to $pHIn_{0.5}$ values of sensory neuron ASICs of ~7.3 [35].

In ENaC, a channel related to ASICs, Na^+ self-inhibition is observed as the exponential current decrease after an initial peak of Na^+ current, similar to open channel inactivation in ASICs [19]. The time course of Na^+ self-inhibition is accelerated with increasing temperature. A study that investigated the temperature dependence of self-inhibition showed that the decrease in ENaC currents observed at higher temperature was due to the increase in the inactivation rate. We observed a pronounced temperature dependence of the time course of open channel inactivation in all ASICs and a significant decrease in peak

current amplitudes of ASIC1a and ASIC1b. The observed decrease in ASIC peak current amplitudes at higher temperature may be in part due to a stronger acceleration of the open channel inactivation rate as compared to the activation rate, similar as in ENaC. To test whether the observed changes in peak current density may be explained by the temperature dependence of the inactivation kinetics, we modeled macroscopic ASIC currents by using a three-state model including a closed, an open, and an inactivated state (see Supplementary Methods, online resource 3). The acid-induced current can be described by two transition rates, representing the closed-to-open and the open-to-inactivated transition, except for ASIC2a that displays a substantial sustained current component at the pH studied and requires, therefore, in addition a rate for the inactivated-to-open transition. To simulate a current trace at 35°C, the open-to-inactivated rate was taken from the exponential fit to open channel inactivation at 35°C while the closed-to-open rate and the unitary conductance (and the inactivated-to-open rate for ASIC2a) were either kept the same as for 25°C, or increased by 1.3-fold (minimal Q10 for diffusion processes). The simulated current traces at 25°C and 35°C are shown in Supplementary Fig. S3 (online resource 4) as interrupted lines, superposed on representative traces. The simulation reproduced the current traces for ASIC1a, ASIC1b, and ASIC3 but not ASIC2a if the closed-to-open transition and the conductance were kept the same as for 25°C. However, it did not predict current decreases if these values were increased by a factor of 1.3. Since the temperature dependence of the opening rate and of the unitary conductance of ASICs is not known, it is not possible to estimate to which extent the observed decrease in peak current amplitude of ASIC1a and ASIC1b at the higher temperature is due to the accelerated open channel inactivation. For ASIC currents in sensory neurons with a $pHIn_{0.5}$ of around 7.3, as well as for cloned ASIC1a with a $pHIn_{0.5}$ of 7.2, the small alkaline shift of $pHIn_{0.5}$ upon temperature increase likely leads to partial inactivation of ASICs and therefore an added current reduction.

Temperature dependence of TRPV1

TRPV1 is activated by diverse stimuli, such as temperature, extracellular protons, voltage, and ligands (reviewed in [25]). There is strong evidence that these different ways of activating TRPV1 interact with each other. It has been shown for the two TRP family members TRPV1 and TRPM8 that they have a strong inherent voltage dependence and that changes in temperature or exposure to low concentrations of activators shift this voltage dependence and thereby activate these channels at physiological negative membrane potentials [48]. In the study by Voets and colleagues, a two-state model was sufficient to describe the activity of TRPV1 and TRPM8 with either the opening rate (TRPV1) or the closing rate (TRPM8) showing a high-temperature dependence. A recent study provided evidence that voltage alone may only be a partial activator and that higher concentrations of agonists activate these channels by voltage-independent mechanisms [28]. These authors proposed an allosteric model of the control of TRPV1 and TRPM8 activity by voltage, temperature, agonists, and antagonists.

Consistent with an allosteric model or a model in which different pathways converge for channel activation, interdependence of the effect of different TRPV1 activators has been shown in many studies. In several cases, one stimulus could affect the concentration dependence of a second stimulus. Extracellular acidification has been shown to shift the TRPV1 concentration–response curve of agonists such as capsaicin and anandamide to lower values and to lower the temperature activation threshold [3, 22, 31, 42, 47]. It was also shown that capsaicin potentiates the heat-induced current in DRG neurons [47]. In studies on H^+-induced TRPV1 currents in DRG neurons as well as in jugular and nodose neurons innervating rat lungs, pH 5.5-induced TRPV1 currents were increased by raising the temperature [32, 33]. We confirm here the increase in current amplitude and show in addition that increasing the temperature accelerates the appearance of the H^+-induced current but does not change the pH dependence of activation.

The observation that pH can modulate the concentration dependence of agonists and the temperature dependence, but that the reverse, regulation of pH dependence by temperature, does not occur, is likely linked to the existence of two proton binding sites with different functions [22]. Jordt and colleagues showed that protons modulate the temperature dependence of temperature activation as well as the concentration dependence of activation by capsaicin, by protonating Glu-600 of TRPV1 with a pH of half-maximal effect of ~7. Glu-600 is, however, a modulatory and not the activator proton binding site in TRPV1, which also has a different pH dependence [22]. TRPV1 activation by pH clearly interacts with the activation by temperature since increasing the temperature affects H^+-induced currents. However, the interaction between the activator proton binding site and other activation pathways is probably not as close as that of the modulatory site, explaining the lack of change in pH dependence when the temperature is raised.

Since the increase in H^+-gated TRPV1 current amplitudes at higher temperature is not due to a change in pH dependence, it must be caused by other mechanisms. We have observed a negative shift in the voltage dependence of the TRPV1 conductance at the higher temperature (Fig. 4g, h), which explains at least in part the observed current increase. Interestingly, we observed besides the shift in

voltage dependence an increase in maximal conductance at 35°C, consistent with observations made for other TRPV1 activators [28]. On the level of the microscopic gating transitions, the changed voltage dependence is expected to affect the transition rates. We have observed an acceleration of the TRPV1 activation kinetics at higher temperature (Fig. 4d) which, in a two-state model as the one described by Voets and colleagues, would reflect an increase of either the opening or closing rate or both [48]. If the opening rate is more increased than the closing rate, this would lead to an increase in open probability, explaining the increased current amplitude at the higher temperature. The available data do not, however, allow confirming or rejecting this hypothesis.

pH sensing in DRG neurons at physiological temperature

Both ASICs and TRPV1 are widely expressed in small diameter DRG neurons. pH-dependent currents mediated by ASICs are induced by pH≤7 with $pH_{0.5}$ values around 6.5–6, while TRPV1 currents have a $pH_{0.5}$ of ~5. At physiological temperature, the situation in small diameter DRG neurons is the following. At pH>6 ASICs mediate alone the pH-induced inward currents. Acidification to pH 6 activates both ASICs and TRPV1. The peak current amplitudes at pH 6 are ≥10-fold higher for ASICs than for TRPV1. At pH<6, the amplitudes of TRPV1 currents further increase with stimulation pH of increasing acidity while the amplitudes of the two main ASIC current types have already reached their maximum at around pH 6. As a consequence, ASIC and TRPV1 currents are of similar amplitude at pH 5 and become greater for TRPV1 at more acidic pH. The ratio of the transported charge follows a similar pH dependence, with greater amplitudes for TRPV1 starting at slightly above pH 5.

This ratio can be changed by two mechanisms of TRPV1 regulation, sensitization, and desensitization. TRPV1 is known to be sensitized in inflammatory conditions. Sensitization is thought to depend on phosphorylation, PiP_2 hydrolysis, or increased expression (reviewed in [39, 41]). Interestingly, sensitization can shift the pH dependence of TRPV1 activation to more alkaline values [43, 46]. Moreover, in inflamed tissue, the temperature can rise above normal levels and can, therefore, further increase the TRPV1 and decrease the ASIC currents. It is, however, important to note that TRPV1 undergoes strong and long-lasting desensitization after repeated or prolonged stimulation, limiting considerably its function as pH sensor [23, 42]. Due to this multitude of possible regulations, the relative contribution to pH sensing in vivo of these two channel types is not easily predictable.

In our experiments, the "TRPV1-like" sustained H^+-induced current was inhibited by BCTC, and all neurons expressing such a current also showed a capsaicin-activated current, thus suggesting that the H^+-induced sustained current was mediated by TRPV1. However, we cannot exclude that a small part of this sustained current is mediated by other pH-sensitive channels shown to be present in sensory neurons, as, e.g., TRPV4 or TRPC4 or TRPC5 [18].

We have studied acid-induced AP generation in DRG neurons at 25°C and 35°C by acidification to pH values between 7 and 6, which mainly activate ASICs. In neurons expressing ASIC type 3 currents, the depolarization amplitude decreased with increasing temperature. Although the decrease in depolarization amplitude and duration at 35°C was not sufficient to change the AP induction significantly in our experiments, it might under different conditions lead to a smaller effect of ASICs on AP generation at 35°C as compared to 25°C.

While the effects of ASIC activity on DRG neuron signaling support a pro-nociceptive role of ASICs that is confirmed by experiments with rodents and humans (see "Introduction"), two studies with mice provided evidence for an anti-nociceptive or modulatory role of ASICs in pain sensation [7, 29]. It is currently not clear under which conditions and in which neurons ASICs may negatively modulate pain perception. However, if such a function can be confirmed in further studies, it is expected to be enforced at lower temperatures due to increased ASIC current amplitudes and the slowing of the open channel inactivation and might thereby contribute to cold-induced pain relief [12].

In conclusion, our study shows that ASICs and TRPV1 that are frequently co-expressed in sensory neurons have distinct functions as pH sensors. At physiological temperature, ASICs are the main pH sensing ion channels for pH≥6 whereas TRPV1 contributes more importantly at more acidic pH. Their differences in current kinetics and ion permeability most likely further define their respective roles.

Acknowledgments We thank Laurent Schild, Aurélien Boillat, Benoîte Bargeton, Cedric Laedermann, Olivier Poirot, and Miguel van Bemmelen for their comments on a previous version of the manuscript and for many discussions. This research was supported by grant 31003A0-117717 of the Swiss National Science Foundation to S.K.

Conflict of interest The authors declare that they have no conflict of interest.

References

1. Askwith CC, Benson CJ, Welsh MJ, Snyder PM (2001) DEG/ENaC ion channels involved in sensory transduction are modulated by cold temperature. Proc Natl Acad Sci USA 98:6459–6463

2. Benson CJ, Xie JH, Wemmie JA, Price MP, Henss JM, Welsh MJ, Snyder PM (2002) Heteromultimers of DEG/ENaC subunits form H^+-gated channels in mouse sensory neurons. Proc Natl Acad Sci USA 99:2338–2343
3. Bianchi BR, Lee CH, Jarvis MF, El Kouhen R, Moreland RB, Faltynek CR, Puttfarcken PS (2006) Modulation of human TRPV1 receptor activity by extracellular protons and host cell expression system. Eur J Pharmacol 537:20–30
4. Blair NT, Bean BP (2002) Roles of tetrodotoxin (TTX)-sensitive Na^+ current, TTX-resistant Na^+ current, and Ca^{2+} current in the action potentials of nociceptive sensory neurons. J Neurosci 22:10277–10290
5. Caterina MJ, Leffler A, Malmberg AB, Martin WJ, Trafton J, Petersen-Zeitz KR, Koltzenburg M, Basbaum AI, Julius D (2000) Impaired nociception and pain sensation in mice lacking the capsaicin receptor. Science 288:306–313
6. Caterina MJ, Schumacher MA, Tominaga M, Rosen TA, Levine JD, Julius D (1997) The capsaicin receptor—a heat-activated ion channel in the pain pathway. Nature 389:816–824
7. Chen C-C, Zimmer A, Sun W-H, Hall J, Brownstein MJ, Zimmer A (2002) A role for ASIC3 in the modulation of high-intensity pain stimuli. PNAS 99:8992–8997
8. Chen X, Paukert M, Kadurin I, Pusch M, Grunder S (2006) Strong modulation by RFamide neuropeptides of the ASIC1b/3 heteromer in competition with extracellular calcium. Neuropharmacology 50:964–974
9. Davis JB, Gray J, Gunthorpe MJ, Hatcher JP, Davey PT, Overend P, Harries MH, Latcham J, Clapham C, Atkinson K, Hughes SA, Rance K, Grau E, Harper AJ, Pugh PL, Rogers DC, Bingham S, Randall A, Sheardown SA (2000) Vanilloid receptor-1 is essential for inflammatory thermal hyperalgesia. Nature 405:183–187
10. Deval E, Baron A, Lingueglia E, Mazarguil H, Zajac JM, Lazdunski M (2003) Effects of neuropeptide SF and related peptides on acid sensing ion channel 3 and sensory neuron excitability. Neuropharmacol 44:662–671
11. Donier E, Rugiero F, Jacob C, Wood JN (2008) Regulation of ASIC activity by ASIC4—new insights into ASIC channel function revealed by a yeast two-hybrid assay. Eur J Neurosci 28:74–86
12. East CE, Begg L, Henshall NE, Marchant P, Wallace K (2007) Local cooling for relieving pain from perineal trauma sustained during childbirth. Cochrane Database Syst Rev: CD006304
13. Escoubas P, DeWeille JR, Lecoq A, Diochot S, Waldmann R, Champigny G, Moinier D, Ménez A, Lazdunski M (2000) Isolation of a tarantula toxin specific for a class of proton-gated Na^+ channels. J Biol Chem 275:25116–25121
14. Gonzales EB, Kawate T, Gouaux E (2009) Pore architecture and ion sites in acid-sensing ion channels and P2X receptors. Nature 460:599–604
15. Good NE, Winget GD, Winter W, Connolly TN, Izawa S, Singh RM (1966) Hydrogen ion buffers for biological research. Biochemistry 5:467–477
16. Hesselager M, Timmermann DB, Ahring PK (2004) pH dependency and desensitization kinetics of heterologously expressed combinations of acid-sensing ion channel subunits. J Biol Chem 279:11006–11015
17. Hille B (2001) Ion channels of excitable membranes. Sinauer Associates, Sunderland
18. Holzer P (2009) Acid-sensitive ion channels and receptors. Handb Exp Pharmacol 194:283–332
19. Horisberger JD, Chraibi A (2004) Epithelial sodium channel: a ligand-gated channel? Nephron Physiol 96:p37–p41
20. Jasti J, Furukawa H, Gonzales EB, Gouaux E (2007) Structure of acid-sensing ion channel 1 at 1.9 A resolution and low pH. Nature 449:316–323
21. Jones NG, Slater R, Cadiou H, McNaughton P, McMahon SB (2004) Acid-induced pain and its modulation in humans. J Neurosci 24:10974–10979
22. Jordt SE, Tominaga M, Julius D (2000) Acid potentiation of the capsaicin receptor determined by a key extracellular site. Proc Natl Acad Sci USA 97:8134–8139
23. Koplas PA, Rosenberg RL, Oxford GS (1997) The role of calcium in the desensitization of capsaicin responses in rat dorsal root ganglion neurons. J Neurosci 17:3525–3537
24. Krishtal O (2003) The ASICs: signaling molecules? Modulators? Trends Neurosci 26:477–483
25. Latorre R, Brauchi S, Orta G, Zaelzer C, Vargas G (2007) ThermoTRP channels as modular proteins with allosteric gating. Cell Calcium 42:427–438
26. Lawson SN, Perry MJ, Prabhakar E, McCarthy PW (1993) Primary sensory neurones: neurofilament, neuropeptides, and conduction velocity. Brain Res Bull 30:239–243
27. Lingueglia E, de Weille JR, Bassilana F, Heurteaux C, Sakai H, Waldmann R, Lazdunski M (1997) A modulatory subunit of acid sensing ion channels in brain and dorsal root ganglion cells. J Biol Chem 272:29778–29783
28. Matta JA, Ahern GP (2007) Voltage is a partial activator of rat thermosensitive TRP channels. J Physiol 585:469–482
29. Mogil JS, Breese NM, Witty M-F, Ritchie J, Rainville M-L, Ase A, Abbadi N, Stucky CL, Seguela P (2005) Transgenic expression of a dominant-negative ASIC3 subunit leads to increased sensitivity to mechanical and inflammatory stimuli. J Neurosci 25:9893–9901
30. Mohan C (2003) Calbiochem buffer guide. EMD Biosciences, Darmstadt
31. Neelands TR, Jarvis MF, Han P, Faltynek CR, Surowy CS (2005) Acidification of rat TRPV1 alters the kinetics of capsaicin responses. Mol Pain 1:28
32. Neelands TR, Zhang XF, McDonald H, Puttfarcken P (2010) Differential effects of temperature on acid-activated currents mediated by TRPV1 and ASIC channels in rat dorsal root ganglion neurons. Brain Res 1329:55–66
33. Ni D, Lee LY (2008) Effect of increasing temperature on TRPV1-mediated responses in isolated rat pulmonary sensory neurons. Am J Physiol Lung Cell Mol Physiol 294:L563–L571
34. Petruska JC, Napaporn J, Johnson RD, Gu JGG, Cooper BY (2000) Subclassified acutely dissociated cells of rat DRG: histochemistry and patterns of capsaicin-, proton-, and ATP-activated currents. J Neurophysiol 84:2365–2379
35. Poirot O, Berta T, Decosterd I, Kellenberger S (2006) Distinct ASIC currents are expressed in rat putative nociceptors and are modulated by nerve injury. J Physiol 576:215–234
36. Poirot O, Vukicevic M, Boesch A, Kellenberger S (2004) Selective regulation of acid-sensing ion channel 1 by serine proteases. J Biol Chem 279:38448–38457
37. Price MP, McIlwrath SL, Xie JH, Cheng C, Qiao J, Tarr DE, Sluka KA, Brennan TJ, Lewin GR, Welsh MJ (2001) The DRASIC cation channel contributes to the detection of cutaneous touch and acid stimuli in mice. Neuron 32:1071–1083
38. Sluka KA, Price MP, Breese NA, Stucky CL, Wemmie JA, Welsh MJ (2003) Chronic hyperalgesia induced by repeated acid injections in muscle is abolished by the loss of ASIC3, but not ASIC1. Pain 106:229–239
39. Stucky CL, Dubin AE, Jeske NA, Malin SA, McKemy DD, Story GM (2009) Roles of transient receptor potential channels in pain. Brain Res Rev 60:2–23
40. Sutherland SP, Benson CJ, Adelman JP, McCleskey EW (2001) Acid-sensing ion channel 3 matches the acid-gated current in cardiac ischemia-sensing neurons. Proc Natl Acad Sci USA 98:711–716

41. Szallasi A, Cortright DN, Blum CA, Eid SR (2007) The vanilloid receptor TRPV1: 10 years from channel cloning to antagonist proof-of-concept. Nat Rev Drug Discov 6:357–372
42. Tominaga M, Caterina MJ, Malmberg AB, Rosen TA, Gilbert H, Skinner K, Raumann BE, Basbaum AI, Julius D (1998) The cloned capsaicin receptor integrates multiple pain-producing stimuli. Neuron 21:531–543
43. Tominaga M, Wada M, Masu M (2001) Potentiation of capsaicin receptor activity by metabotropic ATP receptors as a possible mechanism for ATP-evoked pain and hyperalgesia. Proc Natl Acad Sci USA 98:6951–6956
44. Ugawa S, Ueda T, Ishida Y, Nishigaki M, Shibata Y, Shimada S (2002) Amiloride-blockable acid-sensing ion channels are leading acid sensors expressed in human nociceptors. J Clin Invest 110:1185–1190
45. Valenzano KJ, Grant ER, Wu G, Hachicha M, Schmid L, Tafesse L, Sun Q, Rotshteyn Y, Francis J, Limberis J, Malik S, Whittemore ER, Hodges D (2003) *N*-(4-tertiarybutylphenyl)-4-(3-chloropyridin-2-yl)tetrahydropyrazine-1(2H)-carbox-amide (BCTC), a novel, orally effective vanilloid receptor 1 antagonist with analgesic properties: I. In vitro characterization and pharmacokinetic properties. J Pharmacol Exp Ther 306:377–386
46. Vellani V, Mapplebeck S, Moriondo A, Davis JB, McNaughton PA (2001) Protein kinase C activation potentiates gating of the vanilloid receptor VR1 by capsaicin, protons, heat and anandamide. J Physiol 534:813–825
47. Vlachova V, Lyfenko A, Orkand RK, Vyklicky L (2001) The effects of capsaicin and acidity on currents generated by noxious heat in cultured neonatal rat dorsal root ganglion neurones. J Physiol 533:717–728
48. Voets T, Droogmans G, Wissenbach U, Janssens A, Flockerzi V, Nilius B (2004) The principle of temperature-dependent gating in cold- and heat-sensitive TRP channels. Nature 430:748–754
49. Vukicevic M, Weder G, Boillat A, Boesch A, Kellenberger S (2006) Trypsin cleaves acid-sensing ion channel 1a in a domain that is critical for channel gating. J Biol Chem 281:714–722
50. Vyklicky L, Vlachova V, Vitaskova Z, Dittert I, Kabat M, Orkand RK (1999) Temperature coefficient of membrane currents induced by noxious heat in sensory neurones in the rat. J Physiol 517(Pt 1):181–192
51. Waldmann R, Bassilana F, de Weille J, Champigny G, Heurteaux C, Lazdunski M (1997) Molecular cloning of a non-inactivating proton-gated Na+ channel specific for sensory neurons. J Biol Chem 272:20975–20978
52. Waldmann R, Champigny G, Bassilana F, Heurteaux C, Lazdunski M (1997) A proton-gated cation channel involved in acid-sensing. Nature 386:173–177
53. Wang WZ, Chu XP, Li MH, Seeds J, Simon RP, Xiong ZG (2006) Modulation of acid-sensing ion channel currents, acid-induced increase of intracellular Ca^{2+}, and acidosis-mediated neuronal injury by intracellular pH. J Biol Chem 281:29369–29378
54. Wemmie JA, Price MP, Welsh MJ (2006) Acid-sensing ion channels: advances, questions and therapeutic opportunities. Trends Neurosci 29:578–586
55. Zimmermann M (1983) Ethical guidelines for investigations of experimental pain in conscious animals. Pain 16:109–110